Frontiers in Bioscience Landmark

Front. Biosci. (Landmark Ed) **2026**; 31(11): 52769
https://doi.org/10.31083/FBL52769

Original Research

5-Hydroxytryptamine Promotes Non-Small Cell Lung Cancer Metastasis via Regulation of RPL24

Yan Sun[1,†], Dan Zang[1,†], Mei-Xi Lin[1,†], Xu Han[1], Man Sun[1], Jun Chen[1,*]

[1]Department of Oncology, The Second Hospital of Dalian Medical University, 116021 Dalian, Liaoning, China
*Correspondence: chenjun_dmu@126.com (Jun Chen)
[†]These authors contributed equally.

Academic Editors: Esteban C. Gabazza and Manlio Vinciguerra
Submitted: 9 April 2026 Revised: 29 July 2026 Accepted: 17 August 2026 Published: 4 November 2026

Abstract

Background: Non-small cell lung cancer (NSCLC) is characterized by a poor 5-year survival rate of 25%, primarily due to late-stage diagnosis, treatment resistance, and metastasis. 5-hydroxytryptamine (5-HT, serotonin), which is partially synthesized by gut microbiota, plays a role in tumorigenesis; however, its specific influence on NSCLC metastasis is not clearly understood. This study aimed to elucidate the mechanism through which 5-HT may promote NSCLC metastasis. **Methods:** Quantification of peripheral blood 5-HT levels in NSCLC patients, categorized by the presence or absence of distant metastasis, was conducted using ELISA. Profiling of gut microbiota was performed via metagenomics, with analyses conducted to explore correlations with 5-HT levels. Genome-wide sequencing, quantitative real-time polymerase chain reaction (qRT-PCR), Western blotting, Transwell, and scratch assays were utilized to identify key molecules (Ribosomal protein L24, RPL24) and receptors (5-hydroxytryptamine receptor 3A, HTR3A) in NSCLC cell lines (H1299, A549) and normal bronchial epithelial cell line BEAS-2B. **Results:** Significantly elevated peripheral blood 5-HT levels were observed in patients with distant metastasis compared to those without. Additionally, those patients exhibited distinct gut microbial profiles characterized by increased species richness and diversity, with a positive correlation noted between *Clostridium* spp. abundance and 5-HT levels. RPL24 emerged as a critical downstream mediator. The silencing of RPL24 using siRNA markedly enhanced NSCLC cell migration, invasion, and epithelial-mesenchymal transition (EMT), while overexpression yielded opposing effects, indicating that RPL24 functions as a metastasis suppressor in NSCLC. HTR3A was highly expressed in NSCLC tissues and cell lines compared with adjacent non-tumor tissues and normal bronchial epithelial cells. Co-treatment with 5-HT and 8 μM ondansetron (HTR3A antagonist) restored RPL24 expression and significantly counteracted 5-HT-induced metastasis. **Conclusions:** The elevation of 5-HT, linked to gut microbiota (*Clostridium* spp.), fosters a pro-migratory and pro-invasive phenotype in NSCLC cells via HTR3A, thereby activating the EMT pathway. These findings highlight the potential of HTR3A and RPL24 as novel therapeutic targets for metastatic NSCLC.

Keywords: non-small cell lung cancer; 5-hydroxytryptamine; ribosomal protein L24; HTR3A protein; metastasis

1. Introduction

Non-small cell lung cancer (NSCLC) constitutes over 80% of all lung cancer cases and ranks among the leading causes of cancer-related mortality globally [1,2]. Despite ongoing advancements in diagnostic techniques and treatment strategies, the 5-year survival rate for patients remains unsatisfactory due to the high propensity for metastasis and the frequent occurrence of late-stage diagnoses. Therefore, it is essential to decipher the molecular mechanisms that underpin NSCLC metastasis to improve patient prognosis.

Recently, the involvement of neurotransmitters within the tumor microenvironment has garnered significant interest. As a key biogenic amine, 5-hydroxytryptamine (5-HT, serotonin) extends its functionality beyond the classical scope of neural regulation [3]. Over 90% of 5-HT in the human body is synthesized by enterochromaffin cells located in the gastrointestinal tract, with gut microbiota playing a pivotal regulatory role in this synthesis process [4]. Tryptophan hydroxylase 1 (TPH1) is the rate-limiting enzyme for peripheral 5-HT biosynthesis in intestinal enterochromaffin cells. The microbiota can influence TPH1 expression through various metabolites (e.g., short-chain fatty acids) and may even directly participate in tryptophan metabolism, thereby modulating host systemic 5-HT levels [5,6,7]. This “gut microbiota-5-HT” axis presents a novel framework for understanding tumor progression.

Existing study indicates that 5-HT exerts pro-tumorigenic effects across multiple cancer types via specific receptors, enhancing proliferation and migration while inhibiting apoptosis [8]. Furthermore, ribosomal proteins (RPs) have emerged as potential tumor regulators, with their dysregulated expression linked to the progression of various cancers [9], however, their specific roles in NSCLC and the 5-HT signaling pathway remain largely unexplored. Recent research has highlighted that dysbiosis of that gut and airway microbiota contributes to the initiation and progression of lung cancer through mechanisms involving immune modulation and metabolic reprogramming [10,11]. Nonetheless, the potential role of microbiota-driven 5-HT signaling in NSCLC metastasis remains to be investigated.

Copyright: © 2026 The Author(s). Published by IMR Press.
This is an open access article under the CC BY 4.0 license.

Publisher’s Note: IMR Press stays neutral with regard to jurisdictional claims in published maps and institutional affiliations.

Preliminary studies have indicated that 5-HT fosters migration, invasion, and proliferation in NSCLC cells. Thus, this study examined the alterations in gut microbiota and their correlation with peripheral blood 5-HT levels in NSCLC patients exhibiting distant metastasis. Additionally, the molecular mechanisms by which 5-HT facilitates NSCLC metastasis were explored.

2. Materials and Methods

2.1 Patients and Sample Collection

This study received approval from the Ethics Committee (Ethical Approval No.: KY2024-027-01), with all participants providing written informed consent. A total of 48 treatment-naive patients with primary NSCLC were enrolled and categorized into two groups according to TNM staging: the distant metastasis group (Stage IV: Group M) and the non-distant metastasis group (Stages IA-IIIC: Group N). Inclusion and exclusion criteria are detailed in the **Supplementary Material**.

2.2 Fecal and Blood Sample Collection

Fecal samples were collected prior to any therapeutic intervention, immediately transported in liquid nitrogen, and stored at −80 °C for subsequent analysis. Venous blood samples were drawn into sterile centrifuge tubes and allowed to clot at 37 °C for 1 hour. The clotted samples were centrifuged successively at 3000 rpm and 12,000 rpm for 10 minutes each at room temperature (RT). The serum supernatant was meticulously harvested and aliquoted for long-term storage at −80 °C.

2.3 Cell Culture

The NSCLC cell lines H1299 (ATCC-CRL-5803) and A549 (ATCC-CRM-CCL-185), along with the normal bronchial epithelial cell line BEAS-2B (ATCC-CRL-3588), were procured from the Chinese Academy of Medical Sciences (Beijing, China). All cell lines used in this study were validated by Short Tandem Repeat (STR) profiling and tested negative for mycoplasma contamination. These cells were routinely propagated in RPMI-1640 medium (Cat. No. MA0010; Dalian Meilun Biotechnology Co., Ltd., Dalian, Liaoning, China) supplemented with 10% fetal bovine serum, 100 U/mL penicillin, and 100 µg/mL streptomycin, and were maintained at 37 °C in a humidified incubator with a 5% CO_2 atmosphere. All experiments were performed using cells at passages 5 to 15. For cryopreservation, logarithmic-phase cells were resuspended in serum-free cell cryopreservation medium (Beijing Saiwen Innovation Co., Ltd., Beijing, China) and stored at –80 °C.

2.4 Fecal Metagenomic Sequencing

Fecal metagenomic sequencing was conducted with technical support from Beijing Biomarker Technologies Co., Ltd. (Beijing, China). Genomic DNA was extracted from fecal microbiota using the PowerSoil® DNA Isolation Kit and quantified using a Qubit fluorometer. An appropriate volume of genomic DNA was transferred to a 0.6 mL centrifuge tube, and 1× Tris-EDTA buffer (TE) buffer was added on ice to adjust the final volume to 100 µL. The DNA was sheared to the target fragment size, with fragment size distribution verified by agarose gel electrophoresis. Following shearing, DNA underwent end repair, 3′-end A-tailing, and PCR amplification. After adapter ligation, products were subject to fragment size selection, purification, and stringent library quality control to yield qualified sequencing libraries. The human reference genome sequence was obtained from the NCBI database. Bowtie2 indices were constructed, and Bowtie2 alignment was performed to remove human-derived reads, effectively eliminating host contamination, enriching microbial sequences, and enhancing the signal-to-noise ratio and computational efficiency for subsequent analyses. MEGAHIT was utilized for metagenomic assembly to generate contig sequences for each sample. Based on individual assembly results, coding genes were predicted, and a non-redundant gene set was constructed for downstream analyses.

2.5 Enzyme-Linked Immunosorbent Assay (ELISA)

Serum 5-HT levels were quantified using a commercial human 5-HT ELISA kit (Cat. No. MB-7061A, Meibiao Biotechnology, Jiangsu, China), following the manufacturer's instructions. Samples and standards were added to an antibody-precoated plate and incubated with the horseradish peroxidase (HRP)-conjugated detection antibody. After washing, the signal was developed using the kit's chromogen substrate (Chromogen A and B) and subsequently stopped with the provided solution. Absorbance was measured at 450 nm using a Microplate reader SpectraMax iD5 (Molecular Devices, San Jose, CA, USA), and sample concentrations were determined based on the standard curve.

2.6 GEPIA2 Database Analysis and Whole Transcriptome Sequencing

The Gene Expression Profiling Interactive Analysis 2 (GEPIA2) database (http://gepia2.cancer-pku.cn/#index) was employed to investigate the expression patterns of seven 5-HT receptors in NSCLC tissues, utilizing transcriptome datasets from The Cancer Genome Atlas (TCGA) and Genotype-Tissue Expression (GTEx). The differential expression of HTR3A across various clinical stages of NSCLC, along with its correlation with patient survival prognosis, was the primary focus of this analysis. For whole transcriptome sequencing, total cellular RNA was extracted using TRIzol Reagent. The concentration and purity of RNA samples were quantified with a NanoDrop 2000 spectrophotometer (Thermo Fisher Scientific, Wilmington, DE, USA), while RNA integrity was evaluated using the RNA Nano 6000 Assay Kit on an Agilent 2100 Bioanalyzer. Qualified RNA samples were used to construct tran-

scriptome libraries in accordance with the manufacturer's standard protocols, and sequencing was performed on the Illumina NovaSeq platform. Raw sequencing reads were processed and analyzed through a specialized bioinformatics analysis platform.

2.7 Quantitative Real-Time Polymerase Chain Reaction (qRT-PCR)

Specific primers ((Thermo Fisher Scientific, Waltham, MA, USA); sequences available in **Supplementary Table 1**) were designed to target the genes of interest. Total RNA was extracted from the cells, and samples with an OD260/280 ratio between 1.8 and 2.2 were selected for reverse transcription. The 20 µL reverse transcription system included 4 µL of 5× TransScript® Uni All-in-One SuperMix, 1 µL of genomic DNA (gDNA) Remover, an appropriate amount of RNA, and RNase-free water. The reaction was conducted at 85 °C for 5 minutes and 50 °C for 30 minutes, and the synthesized cDNA was stored at –20 °C for future use. qRT-PCR was performed in 20 µL reactions containing 0.4 µL of each primer, 2 µL of cDNA template, 10 µL of 2× PerfectStart® Green qPCR Supermix (Cat. No. AUQ-01, TransGen Biotech, Beijing, China), and 7.2 µL of nuclease-free water. All samples were run in triplicate using the following cycling program: an initial step at 94 °C for 30 seconds, followed by 40–45 cycles of 94 °C for 5 seconds and 60 °C for 30 seconds.

2.8 Western Blotting

Cell lysis was conducted in RIPA (Radioimmunoprecipitation Assay) buffer supplemented with protease inhibitors, and protein concentrations were determined using a BCA (Bicinchoninic Acid) assay. Equal amounts of protein were resolved by sodium dodecyl sulfate-polyacrylamide gel electrophoresis (SDS-PAGE) on 15% gels and subsequently transferred to polyvinylidene difluoride (PVDF) membranes. After blocking with 5% skim milk, membranes were incubated overnight at 4 °C with primary antibodies against RPL24 (Cat. No. 17082-1-AP, dilution 1:2000, Proteintech, Wuhan, China), β-actin (Cat. No. 58169, dilution 1:1000, Cell Signaling Technology, Danvers, MA, USA), or epithelial-mesenchymal transition (EMT) markers (Cat. No. 9782T, dilution 1:1000, Cell Signaling Technology, Danvers, MA, USA). Following incubation with HRP-conjugated secondary antibodies (Cat. No. AS014, dilution 1:5000, ABclonal, Wuhan, China), protein bands were visualized using an ECL chemiluminescence substrate (Beijing Saiwen Innovation) and captured with a chemiluminescence imaging system.

2.9 Wound Healing and Transwell Assays

For wound healing assays, cells were cultured to confluence in 6-well plates, and a scratch was inflicted using a sterile pipette tip. After washing, cells were maintained in serum-free medium, with wound closure monitored at 0, 24, and 48 hours. In Transwell migration assays, cells were seeded into the upper chamber in serum-free medium, while the lower chamber contained medium with 20% FBS. After 24 hours, migrated cells were fixed, stained with crystal violet, and counted. For invasion assays, Transwell inserts were pre-coated with Matrigel prior to cell seeding, with subsequent steps mirroring those of the migration assay.

2.10 Cell Transfection

Cells were transfected with siRNAs or plasmids (sequences listed in **Supplementary Table 2**) using the jetPRIME reagent following the manufacturer's protocol. In brief, siRNA (final concentration of 20 µM) or plasmid (2 µg) was mixed with the jetPRIME reagent and subsequently added to cells in 6-well plates. After 24 hours, the medium was replaced, and cells were harvested for mRNA or protein analysis at 48 or 72 hours post-transfection, respectively.

2.11 Statistical Analysis

All statistical analyses were performed using GraphPad Prism (Version 9.0.0, GraphPad Software, San Diego, CA, USA; https://www.graphpad.com/scientific-software/prism/), employing two-tailed statistical tests. Normality of data distribution was assessed using the Shapiro-Wilk test, while homogeneity of variances was determined with Levene's test. Comparisons between two groups were analyzed using an unpaired Student's *t*-test. For comparisons involving three or more groups, one-way analysis of variance (ANOVA) was employed. Data are presented as mean ± standard deviation (SD). *In vitro* experiments were based on at least three independent biological replicates. In the clinical cohort analyses, sample sizes for each group are specified in the figure legends. A p-value of less than 0.05 was considered statistically significant.

3. Results

3.1 Gut Microbiota Profiles and Peripheral Blood 5-HT Levels Differ between NSCLC Patients with and without Distant Metastasis

The gut microbiota of NSCLC patients with distant metastasis displays greater species richness and diversity in comparison to those without distant metastasis. Additionally, a positive correlation exists between the abundance of *Clostridium* spp. in the differential microbiota and the peripheral blood 5-HT levels in these patients.

A total of 28 NSCLC patients with distant metastases (Group M, n = 28) and 20 NSCLC patients without distant metastases (Group N, n = 20) were enrolled for this study, with all participants having received no prior pharmacological treatment. The α-diversity of gut microbiota in both groups was analyzed, revealing that the Simpson index, Chaol index, Shannon index, and Abundance-based Coverage Estimator (ACE) index in Group M were significantly higher than those in Group N ($p < 0.05$) (Fig. 1A). β-diversity was assessed using partial least squares-

discriminant analysis (PLS-DA), where the first principal component accounted for 7.01% of the inter-group variance and the second principal component explained 6.13%. The samples from the two groups exhibited a clear trend of separation (Fig. 1B), indicating a distinct overall microbial composition between the groups.

At the phylum level, analysis of gut microbiota structure demonstrated that the dominant phyla in both Group M and Group N included *Firmicutes*, *Bacteroidetes*, and *Proteobacteria*. Among the top 10 phyla by relative abundance, Group M exhibited a higher relative abundance of *Firmicutes* (62% vs. 52%) and *Proteobacteria* (10% vs. 8%) compared to Group N. Conversely, Group M showed a lower relative abundance of *Bacteroidetes* (22% vs. 33%) but a higher relative abundance of *Actinobacteria* (2% vs. 1%) compared to Group N. A Venn diagram illustrating the number of shared and unique phyla indicated a greater number of phyla in Group M (Fig. 1C).

LEfSe analysis of the gut microbiota in both groups identified ten differentially abundant taxa (potential biomarker candidates) at an LDA threshold of 4.0, assessed at multiple taxonomic levels. Specifically, p_*Bacteroidetes*, c_*Bacteroidia*, and o_*Bacteroidales* were enriched in Group N, while f_*Actinomycetaceae*, o_*Actinomycetales*, g_*Subdoligranulum*, f_*Oscillospiraceae*, p_*Firmicutes*, c_*Clostridia*, and o_*Eubacteriales*, were enriched in Group M (Fig. 1D,E). The genus *Clostridium* has been shown to stimulate 5-HT production in the colon through the extensive synthesis of aromatic amines [12], and other research has indicated that *Clostridium* can enhance 5-HT secretion in intestinal enterochromaffin cells [13]. A subsequent correlation analysis between serum 5-HT levels and gut microbiota revealed that 5-HT levels exhibited the strongest positive correlation with *Clostridium* (Fig. 1G), corroborating existing literature findings.

Bacteroidetes and *Firmicutes* are dominant taxa in the human gut microbiota. An analysis of the *Firmicutes*/*Bacteroidetes* ratio in both groups revealed that Group M had a higher *Firmicutes*/*Bacteroidetes* ratio compared to Group N (Fig. 1F). Moreover, ELISA was employed to measure peripheral blood 5-HT levels in both groups, indicating that NSCLC patients with distant metastases exhibited significantly higher peripheral blood 5-HT levels than those without distant metastases ($p < 0.05$, Fig. 1H).

3.2 5-HT Promotes Pro-Migratory and Pro-Invasive Phenotypes of NSCLC Cells by Regulating RPL24

The NSCLC cell line H1299 was divided into two groups: the negative control group (Group NC) and the 5-HT treatment group (Group 5-HT). Group 5-HT was treated with 5-HT at a final concentration of 20 μM for 72 hours, followed by RNA-seq analysis. Gene Ontology (GO) pathway enrichment analysis of differentially expressed genes (DEGs) revealed significant differential enrichment of RP-associated pathways between the two groups (Fig. 2A, Table 1). QRT-PCR assays were conducted to compare the mRNA expression levels of RP-related DEGs between the groups (Fig. 2B).

Table 1. Detailed information on ribosomal protein-related DEGs between group 5-HT and group NC.

Gene ID	Gene symbol	log2 (5-HT / NC)	Qvalue (5-HT / NC)
6152	RPL24	–0.25035	0.002889
6167	RPL37	–0.43938	8.84×10^{-7}
6169	RPL38	–0.48541	1.84×10^{-7}
6171	RPL41	–0.35726	0.001097

Previous literature indicates that RPL24 is associated with well-documented extraribosomal functions in cell cycle regulation and maintenance of the epithelial phenotype, whereas RPL37, RPL38, and RPL41 primarily serve as structural components of the ribosome with limited regulatory roles in tumor metastasis. Consequently, RPL24 was prioritized as the primary candidate for functional validation. Preliminary exploratory assays further demonstrated that RPL24 knockdown had the most pronounced effect on the migratory capacity of NSCLC cells among the four downregulated RPs, thereby reinforcing its selection for further investigation. Subsequently, Western blot analysis was conducted to ascertain the protein expression levels of RPL24 in H1299 and A549 cells following treatment with 5-HT. Compared to the control group, a significant reduction in RPL24 protein expression was observed in NSCLC cells following 5-HT treatment (Fig. 2C). Gene silencing of RPL24 was achieved in the H1299 and A549 NSCLC cell lines using RPL24 small interfering RNA (siRNA). The silencing efficiency was confirmed through qRT-PCR and Western blot experiments, demonstrating successful knockdown of both mRNA and protein levels in the siRNA group relative to the negative control (NC) group (Fig. 2D,E). In subsequent experiments, a wound healing assay was performed to evaluate the effects of transient RPL24 silencing on cell migration in both H1299 and A549 cells. The results revealed that the siRNA group exhibited a significant increase in cell migration at 24 and 48 hours post-scratching compared to the control group (Fig. 2F,G). Additionally, Transwell migration and invasion assays indicated that the number of cells passing through the basement membrane was significantly higher in the siRNA group than in the control group (Fig. 2H,I). These findings suggest that transient silencing of RPL24 markedly enhances the migration and invasion capabilities of H1299 and A549 cells.

RPL24 overexpression was successfully achieved in NSCLC H1299 and A549 cells through transfection with an RPL24-overexpressing plasmid. Both qRT-PCR and Western blot analyses confirmed successful upregulation of RPL24 at the mRNA and protein levels in the overexpres-

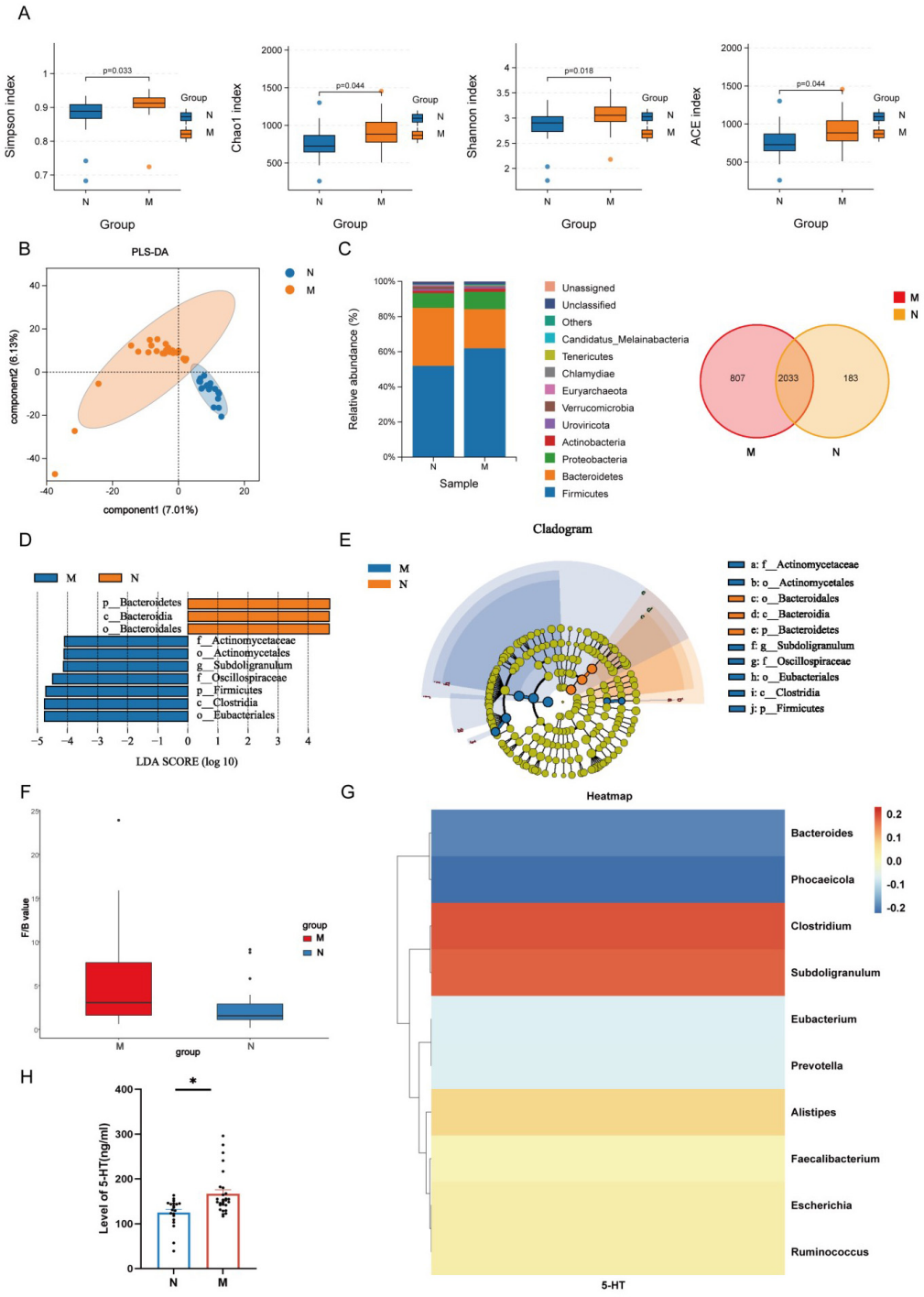


Fig. 1. Gut microbiota characteristics and peripheral blood 5-HT levels in NSCLC patients in Group N and Group M. (A) α-diversity of the gut microbiota. The Simpson, Shannon, Chao1, and ACE indices were significantly higher in Group M than in Group N (all $p < 0.05$). (B) β-diversity analyzed by partial least squares discriminant analysis (PLS-DA). (C) Phylum-level composition of the gut microbiota. (D,E) Linear discriminant analysis effect size (LEfSe) analysis (LDA threshold = 4.0). (D) LDA score plot identifying ten differentially abundant taxa (potential biomarker candidates). (E) Cladogram showing the taxonomic distribution of differentially abundant microbiota. (F) *Firmicutes*/*Bacteroidetes* (F/B) ratio of the gut microbiota in the two groups. (G) Heatmap showing the correlation between serum 5-HT levels and the gut microbiota. (H) Peripheral blood 5-HT levels detected by ELISA. Comparisons between two groups were conducted using Student's *t*-test, with statistical significance defined as $p < 0.05$. Data are presented as mean ± standard deviation (*$p < 0.05$). 5-HT, 5-hydroxytryptamine; NSCLC, non-small cell lung cancer; ACE, Abundance-based Coverage Estimator; LDA, Linear Discriminant Analysis.

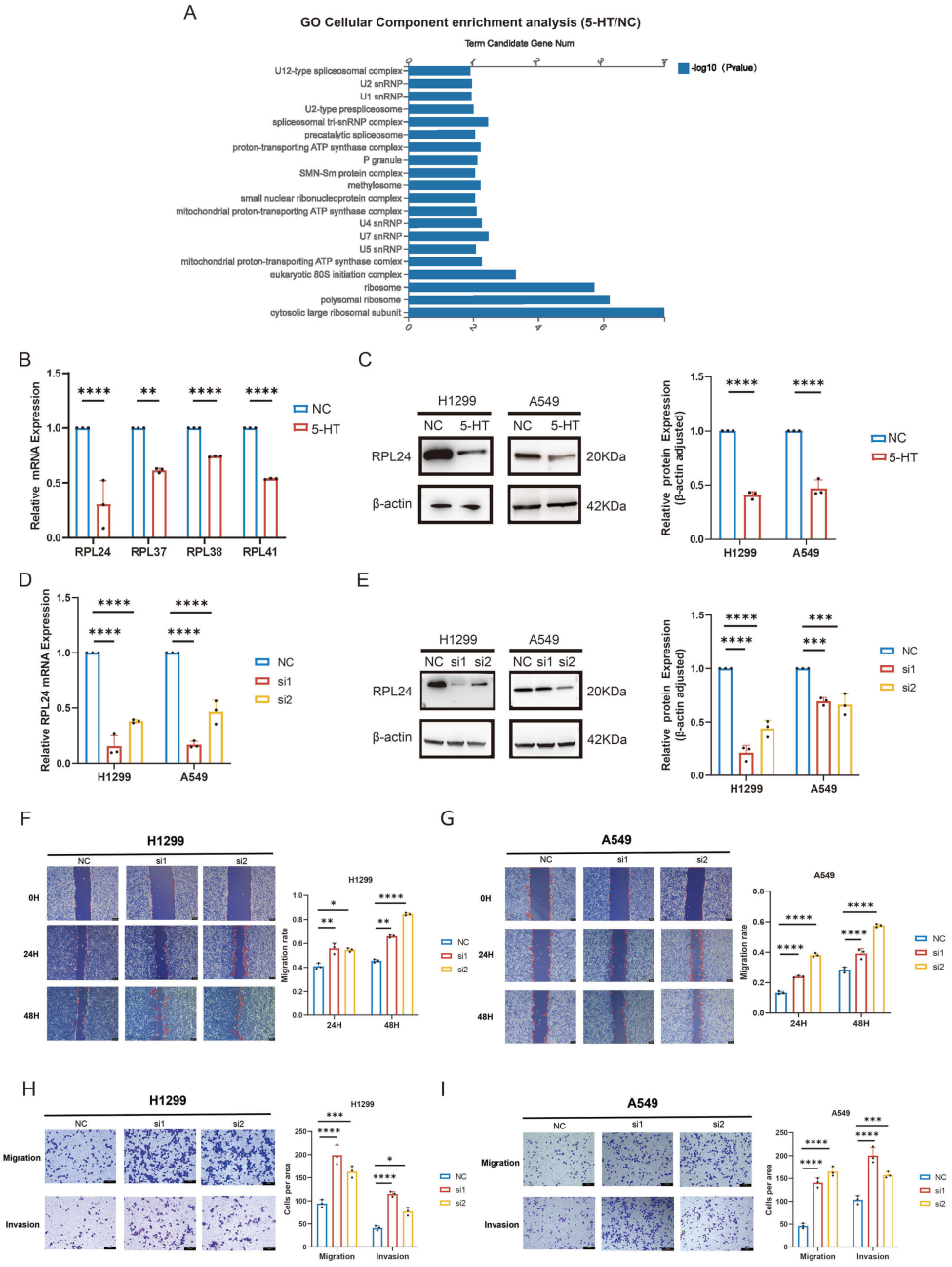


Fig. 2. 5-HT promotes migration and invasion of NSCLC cells by regulating RPL24. (A) GO Cellular Component enrichment analysis of DEGs between Group 5-HT and Group NC. Bubble size indicates the number of candidate genes. (B) qRT-PCR analysis of the mRNA expression levels of ribosomal protein-related DEGs in H1299 and A549 cells. (C) Western blot analysis of RPL24 protein expression in H1299 and A549 cells in the 5-HT and NC groups. (D) qRT-PCR analysis of RPL24 mRNA silencing efficiency in H1299 and A549 cells transfected with RPL24 siRNAs (si1, si2) or negative control (NC). (E) Western blot analysis confirming RPL24 protein silencing efficiency in H1299 and A549 cells transfected with si1, si2, or NC. (F,G) Wound healing assays assessing the migratory capacity of H1299 (F) and A549 (G) cells transfected with si1, si2, or NC. Migration rates were quantified at 24 and 48 h after scratching. Original magnification, 50×. Scale bar = 200 μm. (H,I) Transwell migration and invasion assays showing the numbers of migrated and invaded H1299 (H) and A549 (I) cells transfected with si1, si2, or NC. Original magnification, 100×. Scale bar = 200 μm. Statistical comparisons were made using Student's *t*-test for two-group comparisons and one-way analysis of variance (ANOVA) for multi-group comparisons, with statistical significance set at $p < 0.05$. All data are derived from at least three independent experiments and presented as mean ± standard deviation (*$p < 0.05$, **$p < 0.01$, ***$p < 0.001$, ****$p < 0.0001$). RPL24, Ribosomal Protein L24; GO, Gene Ontology; DEGs, differentially expressed genes; 5-HT, 5-HT treatment group; NC, Negative control group; qRT-PCR, quantitative real-time polymerase chain reaction.

sion (OE) group compared to the empty vector control (Vector) group (Fig. 3A,B). Wound healing assays were conducted to assess the impact of RPL24 overexpression on cell migratory capacity. The results indicated that RPL24 overexpression significantly decreased the migratory area of H1299 and A549 cells at 24 and 48 hours compared to the Vector group ($p < 0.05$, Fig. 3C,D). Additionally, Transwell migration and invasion assays demonstrated that RPL24 overexpression markedly reduced the number of cells passing through the basement membrane in both cell lines compared to the Vector group ($p < 0.05$, Fig. 3E,F). These findings suggest that RPL24 overexpression significantly inhibits the migratory and invasive abilities of NSCLC cells.

Following 24 hours of RPL24 overexpression, NSCLC cells were treated with 5-HT (20 μM) for 72 hours (Group 5-HT + OE). Western blot analysis was conducted to evaluate RPL24 protein expression in Group NC, Group 5-HT, and Group 5-HT + OE. Results indicated that RPL24 protein expression was significantly higher in Group 5-HT + OE compared to Group 5-HT ($p < 0.05$, Fig. 4A). Furthermore, wound healing assays revealed that the migration rates of Group 5-HT + OE at 24 and 48 hours were significantly lower than those of Group 5-HT ($p < 0.05$, Fig. 4B,C). These findings suggest that RPL24 overexpression partially reverses the 5-HT-induced migration of NSCLC cells.

3.3 5-HT Promotes Pro-Migratory and Pro-Invasive Phenotypes of NSCLC Cells by Downregulating RPL24 Through the 5-HT3A Receptor

To evaluate the expression of 5-HT receptors in primary NSCLC tissues and adjacent normal tissues, 5-HT signaling-related receptors were initially predicted using the GEPIA2 database. The results demonstrated a significant upregulation of HTR3A in NSCLC tissues compared to adjacent normal tissues (Fig. 5A). When analyzing HTR3A expression across different NSCLC stages via GEPIA2, no statistically significant differences were observed ($F = 1.06$, $p = 0.364$) (Fig. 5B). Additionally, online survival analysis using GEPIA2 showed that high HTR3A expression was significantly associated with poorer overall survival (OS, HR = 1.5, $p = 0.017$; Fig. 5C) and poorer recurrence-free survival (RFS, HR = 1.5, $p = 0.012$) in NSCLC patients (Fig. 5D). Subsequent qRT-PCR analysis confirmed that HTR3A mRNA expression was markedly elevated in NSCLC cell lines (H1299 and A549) compared to normal human bronchial epithelial BEAS-2B cells (Fig. 5E). These findings suggest that HTR3A is a key 5-HT receptor involved in the progression of NSCLC.

To ascertain whether 5-HT exerts its pro-metastatic effects specifically through the HTR3A receptor, A549 and H1299 cells were treated with the HTR3A antagonist ondansetron (8 μM) in combination with 20 μM 5-HT for 72 hours. Western blot analysis was employed to detect changes in RPL24 protein expression. The results indicated that co-treatment with 8 μM ondansetron and 20 μM 5-HT effectively reversed the 5-HT-induced decrease in RPL24 protein expression (Fig. 5F,G). Following this, Transwell migration/invasion assays and wound healing assays were performed on A549 and H1299 cells post-treatment. The results demonstrated that 5-HT significantly enhanced the migration and invasion of A549 and H1299 cells compared to the blank control group; however, this effect was attenuated by the addition of ondansetron (Fig. 5H–K). These findings indicate that 5-HT promotes a pro-migratory and pro-invasive phenotype in NSCLC cells by activating the HTR3A receptor to regulate RPL24.

4. Discussion

One major cause of mortality in NSCLC is its high propensity for metastasis and recurrence, which also limits the efficacy of current standard treatments [14,15]. Accumulating evidence has elucidated the roles of 5-HT and its metabolites in modulating multiple hallmarks of tumor progression [16]. Although 5-HT metabolic reprogramming has been reported in various tumor types, existing study primarily focuses on colorectal, pancreatic, and breast cancers, with limited research addressing NSCLC and unclear mechanisms underlying 5-HT-induced metastasis in this context [17]. In breast cancer, advanced stages of the disease are associated with significantly higher plasma 5-HT levels compared to early-stage patients, suggesting a correlation with malignant progression [18]. Furthermore, distinct 5-HT levels have been observed in peripheral blood and tissues of colorectal cancer patients in comparison to healthy controls, highlighting its diagnostic potential [19]. Traditional theories of tumor metastasis have predominantly emphasized "intrinsic drivers", such as gene mutations, copy number variations, and epigenetic alterations. However, a recent study demonstrates that neurotransmitters can facilitate metastatic progression in the absence of substantial genomic alterations, thereby challenging the conventional "gene mutation-centric" paradigm [20]. This process, independent of changes in DNA sequences, can be stably transmitted to progeny cells, constituting a non-heritable mechanism that drives metastasis. Preliminary data indicate that treatment-naive NSCLC patients with distant metastasis exhibit higher peripheral blood 5-HT levels, suggesting that 5-HT may serve as a candidate biomarker warranting further investigation.

Most human 5-HT is synthesized in the gastrointestinal tract, with gut microbiota playing a pivotal regulatory role, a landmark study demonstrating that spore-forming gut bacteria are critical regulators of host peripheral 5-HT homeostasis: these commensal bacteria promote 5-HT biosynthesis in colonic enterochromaffin cells via microbial-derived metabolites, and consequently increase 5-HT levels in both the colonic lumen and circulating blood [21,22]. Metagenomic analysis of the gut microbiota in NSCLC has revealed differences in species abundance and

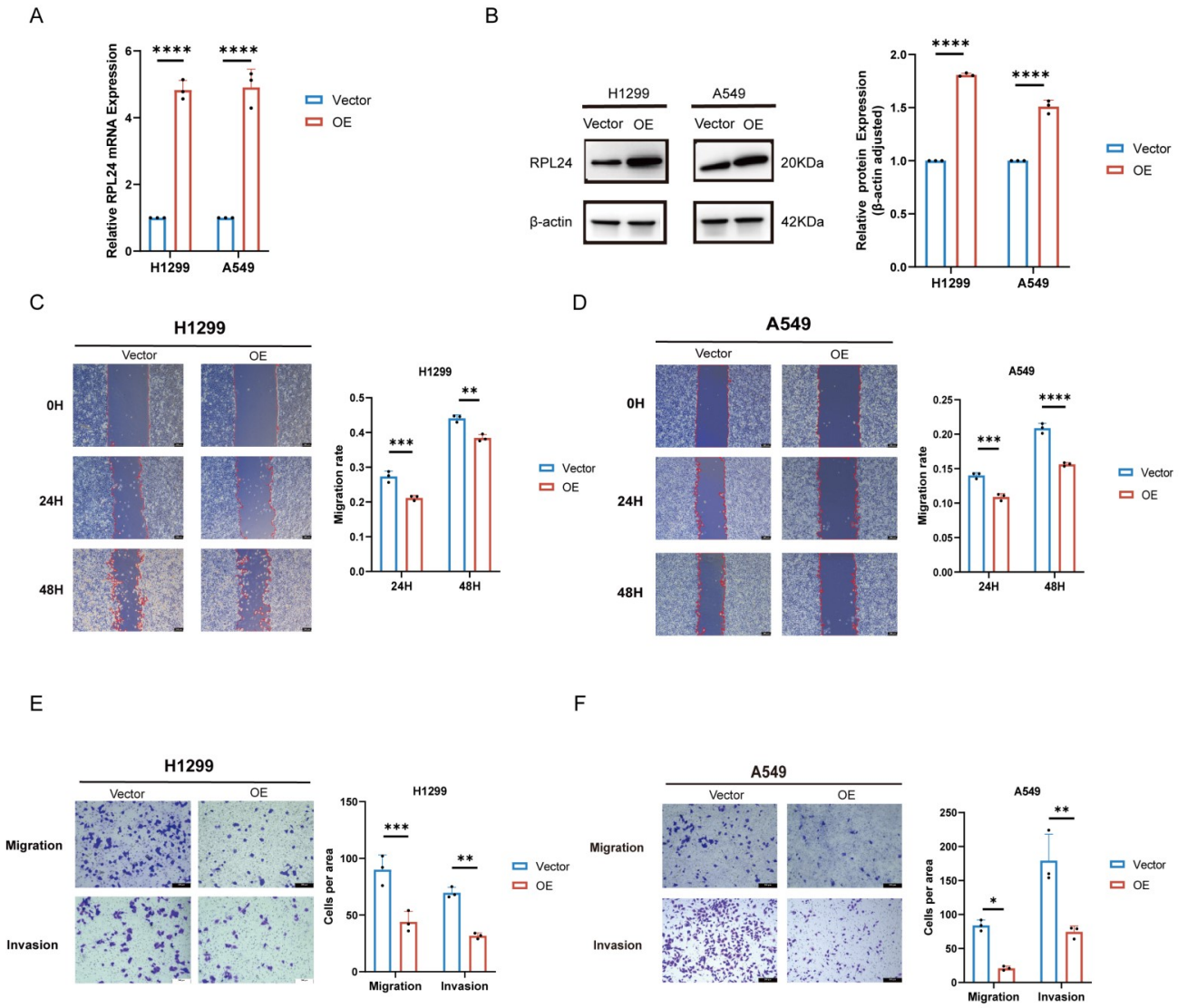


Fig. 3. RPL24 overexpression inhibits the migration and invasion of NSCLC cells. (A) qRT-PCR analysis of RPL24 mRNA expression in Group Vector and Group OE. (B) Western blot analysis of RPL24 protein expression in Group Vector and Group OE. (C,D) Wound healing assays assessing the migratory capacity of H1299 (C) and A549 (D) cells (Group Vector vs. Group OE). Migration rates were quantified at 24 and 48 h after scratching. Original magnification, 50×. Scale bar = 200 μm. (E,F) Transwell migration and invasion assays showing the numbers of migrated and invaded H1299 (E) and A549 (F) cells (Group Vector vs. Group OE). Original magnification, 100×. Scale bar = 200 μm. Statistical comparisons were made using Student's *t*-test for two-group comparisons, with statistical significance defined as $p < 0.05$. All data are derived from at least three independent experiments and presented as mean ± standard deviation (*$p < 0.05$, **$p < 0.01$, ***$p < 0.001$, ****$p < 0.0001$). OE, overexpression.

diversity between metastatic and non-metastatic groups, leading to the identification of ten differentially abundant taxa that warrant further exploration as potential biomarkers. Notably, the abundance of *Clostridium* was positively correlated with peripheral blood 5-HT levels. This finding is consistent with previous reports indicating that *Clostridium* species can induce secretion of 5-HT from intestinal enterochromaffin cells via aromatic amine metabolites and modulation of tryptophan metabolism. Our correlation data support a potential causal role for gut *Clostridium* in elevating circulating 5-HT levels in metastatic NSCLC patients [23,24]. At the phylum level, metastatic patients exhibited an elevated *Firmicutes*/*Bacteroidetes* ratio, consistent with a previous study showing that gut dysbiosis contributes to lung cancer progression via immune and metabolic pathways, our findings further link metastasis-associated microbial alterations to circulating 5-HT levels [25]. Nevertheless, the current observational clinical data only demonstrate a correlation; direct evidence for microbiota-driven elevation of 5-HT in NSCLC necessitates further validation through methodologies such as fecal microbiota transplantation or germ-free animal models.

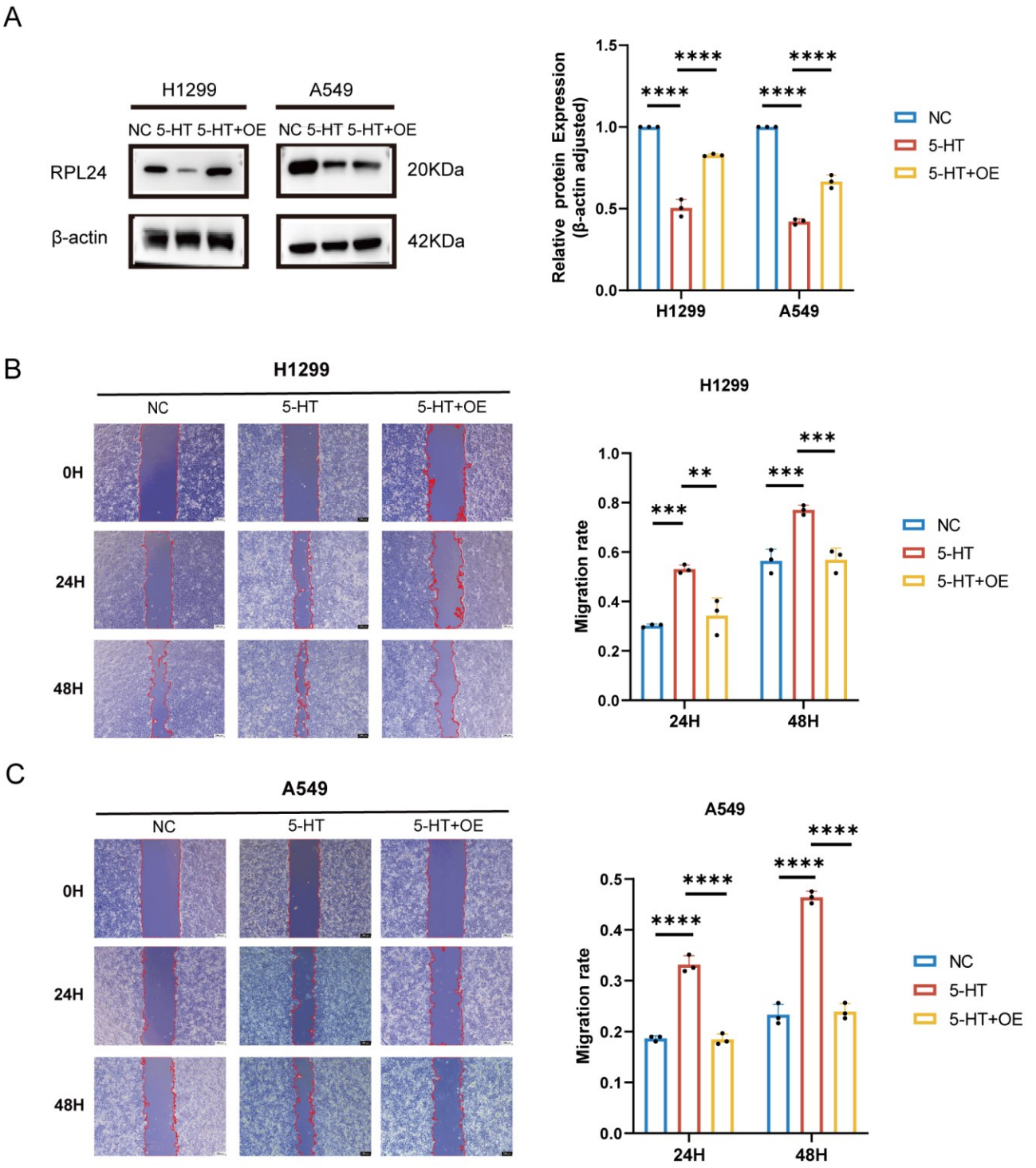


Fig. 4. RPL24 overexpression partially reverses 5-HT-induced migration of NSCLC cells. (A) Western blot analysis of RPL24 protein expression in H1299 and A549 cells in Group NC, Group 5-HT, and Group 5-HT + OE. (B,C) Wound healing assays assessing the migratory capacity of H1299 (B) and A549 (C) cells in Group NC, Group 5-HT, and Group 5-HT + OE. Migration rates were quantified at 24 and 48 h after scratching. Original magnification, 50×. Scale bar = 200 μm. One-way ANOVA was used for multi-group comparisons, with statistical significance defined as $p < 0.05$. All data are derived from at least three independent experiments and presented as mean ± standard deviation (**$p < 0.01$, ***$p < 0.001$, ****$p < 0.0001$).

Traditionally, RPs have been primarily regarded as executors of protein synthesis. However, recent studies have gradually revealed that certain RPs also possess "extraribosomal functions", taking on more diverse roles in cellu-

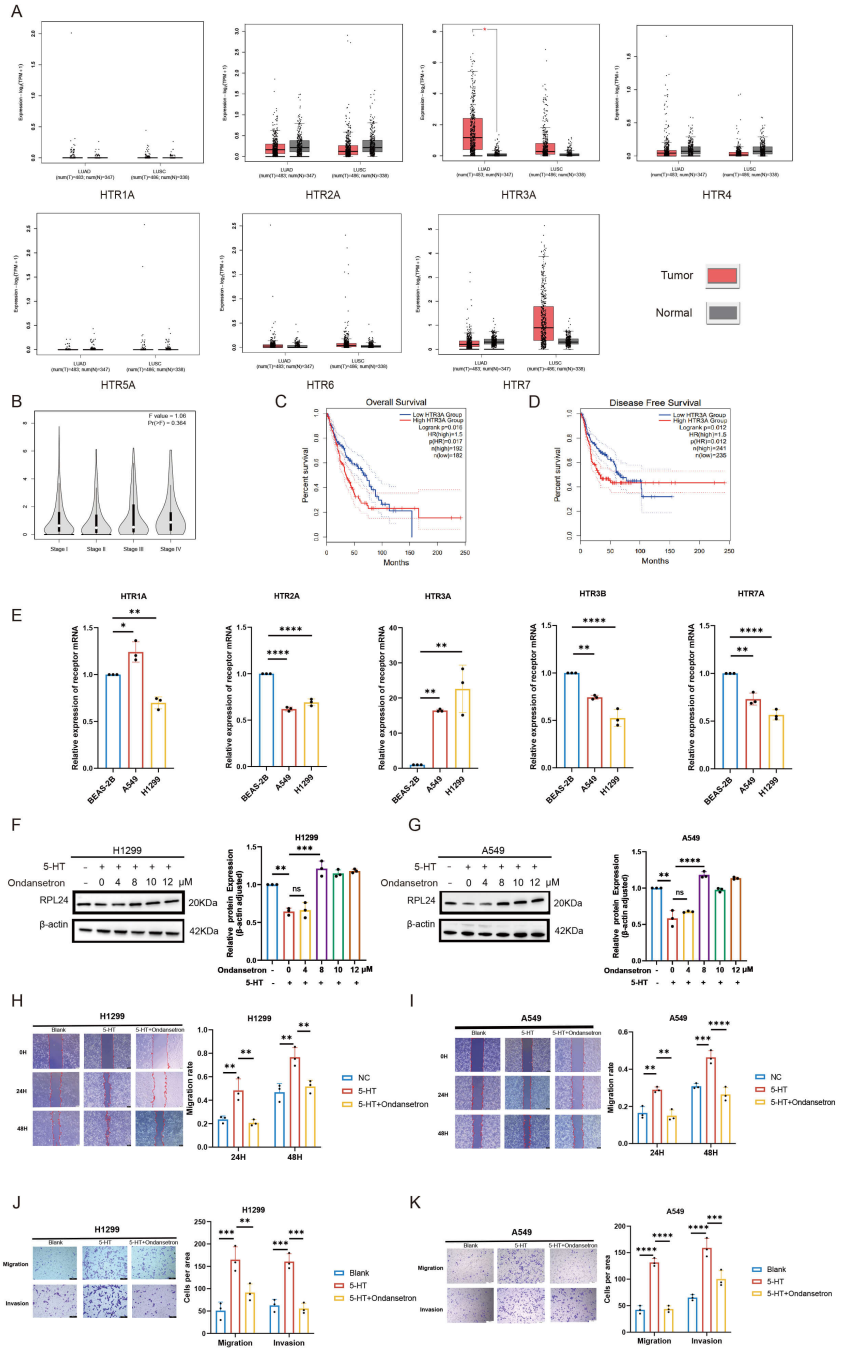


Fig. 5. HTR3A is a key 5-HT receptor mediating the 5-HT-induced pro-migratory and pro-invasive phenotype in NSCLC cells by regulating RPL24. (A) GEPIA2 database analysis of 5-HT receptor expression in primary NSCLC tissues and adjacent normal tissues. (B) GEPIA2-based analysis of HTR3A expression across different NSCLC stages ($p = 0.364$). (C,D) GEPIA2-based online survival analysis showing the association of HTR3A expression with OS ($p = 0.017$) and RFS ($p = 0.012$) in NSCLC patients. (E) qRT-PCR analysis of HTR3A mRNA expression in H1299, A549, and BEAS-2B cells. (F,G) Western blot analysis of RPL24 protein expression in H1299 (F) and A549 (G) cells treated with 5-HT alone or in combination with ondansetron for 72 h. (H,I) Wound healing assays assessing the migratory capacity of H1299 (H) and A549 (I) cells in the NC, 5-HT-treated, and 5-HT + ondansetron groups. Original magnification, 50×. Scale bar = 200 μm. (J,K) Transwell migration and invasion assays showing the migratory and invasive capacities of H1299 (J) and A549 (K) cells in the NC, 5-HT-treated, and 5-HT + ondansetron groups. Original magnification, 100×. Scale bar = 200 μm. Student's *t*-test was used for two-group comparisons, and one-way ANOVA was used for multiple-group comparisons. Statistical significance was defined as $p < 0.05$. All data are derived from at least three independent experiments and are presented as mean ± standard deviation (ns, not significant; *$p < 0.05$, **$p < 0.01$, ***$p < 0.001$, ****$p < 0.0001$). HTR3A, 5-hydroxytryptamine receptor 3A; GEPIA2, Gene Expression Profiling Interactive Analysis 2; OS, overall survival; RFS, recurrence-free survival.

IMR Press

lar activities [9,26]. RPL24, a member of the ribosomal protein L24E family, is an essential component of the 60S ribosomal subunit in eukaryotic cells. Accumulating evidence indicates that RPs not only participate in ribosome assembly and mediate protein biosynthesis but also extensively regulate other cellular processes, with their roles in tumorigenesis and progression attracting increasing attention. For example, RPL24 depletion has been shown to suppress colorectal tumorigenesis by inhibiting translation elongation [27], and RPL24 expression is associated with prognosis in cervical cancer patients [9]. Nevertheless, the specific role of RPL24 in lung cancer progression remains poorly understood. Through whole-transcriptome sequencing screening, this study identified RPL24 as a potential downstream target of 5-HT signaling regulation. A previous study suggests that RPL24 depletion has minimal impact on the basic physiological functions of ribosomes [28], prompting investigations into its functions through RPL24 gene knockdown and overexpression experiments in NSCLC cells. The results demonstrated that transient silencing of RPL24 significantly enhanced, while overexpression inhibited, the migration and invasion abilities of NSCLC cells, indicating a tumor-suppressive role of RPL24 in NSCLC metastasis. Importantly, the role of RPL24 appears context-dependent across different cancer types: whereas upregulation of RPL24 correlates with poor prognosis in cervical cancer [9], the present data and recent pan-cancer analyses suggest a metastasis-suppressive function in lung epithelial malignancies, potentially reflecting tissue-specific translational regulatory networks. Collectively, the data presented demonstrate that EMT is a core downstream consequence of HTR3A/RPL24 axis activation by 5-HT [29]. While acknowledging that 5-HT may also modulate EMT through additional parallel signaling pathways (e.g., ERK or PI3K/Akt pathways) via other 5-HT receptor subtypes, the near-complete reversal of 5-HT-induced EMT and metastasis via RPL24 overexpression indicates that the HTR3A-RPL24 cascade serves as the dominant mediator in this experimental context. Additionally, other RPs concurrently downregulated by 5-HT, such as RPL37, RPL38, and RPL41, may also contribute to the pro-metastatic phenotype, and their individual roles in NSCLC progression warrant further investigation in future studies.

Notably, A549 and H1299 are NSCLC lines not derived from metastatic lesions, yet ondansetron inhibited 5-HT-induced RPL24 downregulation via HTR3A in both, indicating this pathway is a general feature of NSCLC cells rather than metastasis-restricted. Its preferential relevance to metastasis therefore remains inferential.

5-HT plays multiple roles in tumor biology through receptor-mediated signal transduction. The known 5-HT receptors are classified into seven families, further subdivided into at least 14 subtypes. By binding to these specific receptors, 5-HT exerts significant effects on tumorigenesis, progression, and the regulation of the tumor immune microenvironment. For example, in colorectal cancer, 5-HT binds to receptors on cancer cells, driving cell proliferation, migration, and invasion by activating the Axin1/β-catenin/MMP-7 signaling axis [30]. In gastric adenocarcinoma, the 5-HT receptor HTR2B is significantly upregulated and promotes disease progression through the PI3K/Akt/mTOR pathway [31]. Li et al. [32] demonstrated that autocrine activation of serotonin receptors on tumor-infiltrating $CD8^+$ T cells enhances antitumor immunity. Importantly, in lung adenocarcinoma, HTR3A expression correlates with poor histological prognosis, and its pro-proliferative effects may be linked to ERK phosphorylation, suggesting that HTR3A antagonists, such as ondansetron, could serve as potential therapeutic strategies for this disease [33].

Findings from this study extend prior work by Tone et al. [33], who demonstrated that HTR3A promotes proliferation through ERK phosphorylation in lung adenocarcinoma, by identifying RPL24 as a novel downstream mediator of 5-HT/HTR3A signaling and connecting this pathway to the gut microbiota–5-HT axis. Recent studies have shown that dysbiosis of gut and airway microbiota contributes to lung cancer initiation and progression through immune modulation and metabolic reprogramming [34]; however, the role of microbiota-driven 5-HT signaling in NSCLC metastasis has not been previously explored, highlighting the novelty of the proposed gut microbiota/5-HT/HTR3A/RPL24/EMT axis.

Based on this background, bioinformatics analysis of potential 5-HT receptor targets was performed using the GEPIA2 database. The results indicated significant upregulation of HTR3A expression in NSCLC tissue samples compared to non-cancerous lung tissues, with high expression closely associated with poor patient prognosis. To verify these findings, mRNA expression levels of 5-HT receptors were assessed in NSCLC cell lines (H1299 and A549) through qRT-PCR, confirming that HTR3A expression in NSCLC cells was significantly higher than in normal bronchial epithelial BEAS-2B cells, in line with the bioinformatics analysis. Functional rescue experiments revealed that combined ondansetron administration at 8 μM effectively antagonized the 5-HT-induced pro-metastatic effect, significantly reducing cancer cell metastatic capacity compared to 5-HT treatment alone. According to the IUPHAR/BPS (International Union of Basic and Clinical Pharmacology /the British Pharmacological Society) Guide to Pharmacology, ondansetron has a pA_2 value of 7.9–8.3 for the human homomeric HT3A receptor, corresponding to nanomolar-range antagonist affinity [35]. The micromolar concentration used in this study exceeds the receptor affinity by three orders of magnitude, which ensures sustained full receptor occupancy. Notably, the 8 μM concentration used in *in vitro* assays falls within the clinically achievable pharmacological range: peak plasma concentrations of ondansetron after standard clinical intravenous or oral dosing

(8–32 mg/day) reach approximately 0.5–3 μM, with local tissue concentrations in the tumor microenvironment potentially higher due to drug accumulation and tissue penetration [36]. This dose-dependent inhibitory effect supports the translational potential of repurposing ondansetron as an adjuvant anti-metastatic agent for NSCLC patients exhibiting high circulating 5-HT levels. These results not only reinforce the critical role of HTR3A in NSCLC progression but also provide experimental evidence for its potential as a therapeutic target.

Our findings carry potential implications for the clinical management of NSCLC patients undergoing immunotherapy. Specifically, we propose that circulating 5-HT levels and gut microbial signatures, particularly *Clostridium* abundance, may serve as non-invasive biomarkers to identify patients at heightened risk of metastasis before or during immunotherapy. Moreover, excessive 5-HT signaling may contribute to an immunosuppressive tumor microenvironment, suggesting that HTR3A inhibition could enhance the efficacy of immune checkpoint blockade. Given that ondansetron, an FDA-approved (U.S. Food and Drug Administration) HTR3A antagonist, is already widely used clinically with a well-established safety profile, repurposing this agent as an adjunct to immunotherapy represents a viable translational strategy. This notion is further supported by a preclinical study demonstrating the feasibility of targeting 5-HT receptors in other cancer types, such as breast cancer [37]. Future prospective clinical trials are warranted to evaluate whether serum 5-HT and HTR3A expression can predict immunotherapy response or guide patient stratification.

Strategies aimed at modulating gut microbiota, such as targeted probiotics or dietary tryptophan modulation, may serve as supportive interventions to reduce systemic 5-HT levels and suppress metastatic progression. Establishing a dynamic biomarker system based on the specific abundance of fecal microbiota, peripheral blood 5-HT levels, and tumoral RPL24 expression will facilitate more accurate patient risk stratification, prediction of therapy response, and real-time monitoring of therapeutic efficacy [38]. Ultimately, this interdisciplinary research pathway, which integrates microbiomics, neurotransmitter signaling, and tumor biology, is expected not only to optimize the treatment paradigm for metastatic NSCLC but also to advance the emerging frontier of the Gut-Nerve-Tumor Axis, providing a novel systematic framework for the prevention and treatment of solid tumor metastasis.

5. Limitations

Several limitations of this study should be acknowledged. First, the cross-sectional design comparing early-stage (IA) with stage IV NSCLC cannot establish causality between gut microbiota alterations and metastasis; the observed differences may reflect, contribute to, or result from the metastatic state. Longitudinal studies and interventional approaches (e.g., fecal microbiota transplantation in animal models) are necessary to establish causality. Second, the clinical cohort was relatively small (n = 48), and potential confounders (diet, antibiotics, comorbidities, prior therapies) were not systematically controlled; no independent validation cohort or formal diagnostic performance assessment was performed. Third, histological subtype information (lung adenocarcinoma vs. squamous cell carcinoma) was unavailable for stratified analysis, limiting generalizability given biological differences between Lung Adenocarcinoma (LUAD) and Lung Squamous Cell Carcinoma (LUSC). Fourth, functional experiments were conducted in established NSCLC cell lines (A549 and H1299) using *in vitro* 2D assays (wound healing and Transwell) that capture only selected steps of the metastatic cascade; *in vivo* metastasis models (e.g., tail vein injection or orthotopic xenografts) are required to validate the pro-metastatic role of the 5-HT/HTR3A/RPL24 axis in a physiological context. Finally, the species-level taxonomic resolution of *Clostridium* spp. in metagenomic sequencing necessitates cautious interpretation. Future studies with larger, prospectively recruited multi-center cohorts incorporating histological subtype stratification, comprehensive metadata, and independent validation are essential to confirm and extend these findings.

6. Conclusion

In summary, our study demonstrates that elevated circulating 5-HT is associated with metastatic NSCLC and promotes pro-migratory and pro-invasive phenotypes through activation of the HTR3A-RPL24 signaling axis. These findings provide mechanistic insight into the gut microbiota/5-HT/tumor interaction network and identify HTR3A and RPL24 as potential therapeutic targets.

Availability of Data and Materials

The datasets generated during and analyzed during the current study are available from the corresponding author on reasonable request.

Author Contributions

YS, DZ, ML, XH, MS, and JC contributed to the study conception and design. YS was mainly responsible for writing the original draft and investigation of the manuscript. ML participated in data curation and editing of the article. DZ provided review and editing for the article. JC participated in the conceptualization and funding acquisition of the article. All authors contributed to editorial changes in the manuscript. All authors read and approved the final manuscript. All authors have participated sufficiently in the work and agreed to be accountable for all aspects of the work.

Ethics Approval and Consent to Participate

The study was conducted in accordance with the Declaration of Helsinki, and approved by the Ethics Committee of the Second Hospital of Dalian Medical University (protocol code KY2024-027-01). Written informed consent was obtained from all participants involved in this study.

Acknowledgment

The graphical abstract was created using BioRender.com.

Funding

This work was supported by the National Natural Science Foundation of China (82203056) and the United Foundation for Dalian Institute of Chemical Physics, Chinese Academy of Sciences and the Second Hospital of Dalian Medical University (DMU-2&DICP UN202505).

Conflicts of Interest

The authors declare no conflicts of interest.

Supplementary Material

Supplementary material associated with this article can be found, in the online version, at https://doi.org/10.31083/FBL52769.

References

[1] Wu J, Lin Z. Non-Small Cell Lung Cancer Targeted Therapy: Drugs and Mechanisms of Drug Resistance. International Journal of Molecular Sciences. 2022; 23: 15056. https://doi.org/10.3390/ijms232315056

[2] Huang Q, Li Y, Huang Y, Wu J, Bao W, Xue C, et al. Advances in molecular pathology and therapy of non-small cell lung cancer. Signal Transduction and Targeted Therapy. 2025; 10: 186. https://doi.org/10.1038/s41392-025-02243-6

[3] Sauma S, Casaccia P. Does the gut microbiota contribute to the oligodendrocyte progenitor niche? Neuroscience Letters. 2020; 715: 134574. https://doi.org/10.1016/j.neulet.2019.134574

[4] Șchiopu CG, Ștefănescu C, Boloș A, Diaconescu S, Gilca-Blanariu GE, Ștefănescu G. Functional Gastrointestinal Disorders with Psychiatric Symptoms: Involvement of the Microbiome-Gut-Brain Axis in the Pathophysiology and Case Management. Microorganisms. 2022; 10: 2199. https://doi.org/10.3390/microorganisms10112199

[5] Côté F, Thévenot E, Fligny C, Fromes Y, Darmon M, Ripoche MA, et al. Disruption of the nonneuronal tph1 gene demonstrates the importance of peripheral serotonin in cardiac function. Proceedings of the National Academy of Sciences of the United States of America. 2003; 100: 13525–13530. https://doi.org/10.1073/pnas.2233056100

[6] Li K, Wei W, Xu C, Lian X, Bao J, Yang S, et al. Prebiotic inulin alleviates anxiety and depression-like behavior in alcohol withdrawal mice by modulating the gut microbiota and 5-HT metabolism. Phytomedicine: International Journal of Phytotherapy and Phytopharmacology. 2024; 135: 156181. https://doi.org/10.1016/j.phymed.2024.156181

[7] Pan M, Qian C, Huo S, Wu Y, Zhao X, Ying Y, et al. Gut-derived lactic acid enhances tryptophan to 5-hydroxytryptamine in regulation of anxiety via *Akkermansia muciniphila*. Gut Microbes. 2025; 17: 2447834. https://doi.org/10.1080/19490976.2024.2447834

[8] Zhang J, Guo Z, Xie Q, Zhong C, Gao X, Yang Q. Tryptophan hydroxylase 1 drives glioma progression by modulating the serotonin/L1CAM/NF-κB signaling pathway. BMC Cancer. 2022; 22: 457. https://doi.org/10.1186/s12885-022-09569-2

[9] Ming C, Bai X, Zhao L, Yu D, Wang X, Wu Y. RPL24 as a potential prognostic biomarker for cervical cancer treated by Cisplatin and concurrent chemoradiotherapy. Frontiers in Oncology. 2023; 13: 1131803. https://doi.org/10.3389/fonc.2023.1131803

[10] Liu NN, Ma Q, Ge Y, Yi CX, Wei LQ, Tan JC, et al. Microbiome dysbiosis in lung cancer: from composition to therapy. NPJ Precision Oncology. 2020; 4: 33. https://doi.org/10.1038/s41698-020-00138-z

[11] Jin C, Lagoudas GK, Zhao C, Bullman S, Bhutkar A, Hu B, et al. Commensal Microbiota Promote Lung Cancer Development via γδ T Cells. Cell. 2019; 176: 998–1013.e16. https://doi.org/10.1016/j.cell.2018.12.040

[12] Sugiyama Y, Mori Y, Nara M, Kotani Y, Nagai E, Kawada H, et al. Gut bacterial aromatic amine production: aromatic amino acid decarboxylase and its effects on peripheral serotonin production. Gut Microbes. 2022; 14: 2128605. https://doi.org/10.1080/19490976.2022.2128605

[13] Wang J, Qiu F, Zhang Z, Liu Y, Zhou Q, Dai S, et al. Clostridium butyricum Alleviates DEHP Plasticizer-Induced Learning and Memory Impairment in Mice via Gut-Brain Axis. Journal of Agricultural and Food Chemistry. 2023; 71: 18524–18537. https://doi.org/10.1021/acs.jafc.3c03533

[14] Miao D, Zhao J, Han Y, Zhou J, Li X, Zhang T, et al. Management of locally advanced non-small cell lung cancer: State of the art and future directions. Cancer Communications (london, England). 2024; 44: 23–46. https://doi.org/10.1002/cac2.12505

[15] Rodrigues G, Higgins KA, Rimner A, Amini A, Chang JY, Chun SG, et al. American Radium Society Appropriate Use Criteria for Unresectable Locally Advanced Non-Small Cell Lung Cancer. JAMA Oncology. 2024; 10: 799–806. https://doi.org/10.1001/jamaoncol.2024.0294

[16] Chan YL, Lai WC, Chen JS, Tseng JTC, Chuang PC, Jou J, et al. TIAM2S Mediates Serotonin Homeostasis and Provokes a Pro-Inflammatory Immune Microenvironment Permissive for Colorectal Tumorigenesis. Cancers. 2020; 12: 1844. https://doi.org/10.3390/cancers12071844

[17] Ye D, Xu H, Tang Q, Xia H, Zhang C, Bi F. The role of 5-HT metabolism in cancer. Biochimica Et Biophysica Acta. Reviews on Cancer. 2021; 1876: 188618. https://doi.org/10.1016/j.bbcan.2021.188618

[18] Zhan D, Wang X, Zheng Y, Wang S, Yang B, Pan B, et al. Integrative dissection of 5-hydroxytryptamine receptors-related signature in the prognosis and immune microenvironment of breast cancer. Frontiers in Oncology. 2023; 13: 1147189. https://doi.org/10.3389/fonc.2023.1147189

[19] Gao R, Wu C, Zhu Y, Kong C, Zhu Y, Gao Y, et al. Integrated analysis of colorectal cancer reveals cross-cohort gut microbial signatures and associated serum metabolites. Gastroenterology. 2022; 163: 1024–1037. https://doi.org/10.1053/j.gastro.2022.06.069

[20] Brown KM, Nair JK, Janas MM, Anglero-Rodriguez YI, Dang LTH, Peng H, et al. Expanding RNAi therapeutics to extrahepatic tissues with lipophilic conjugates. Nature Biotechnology. 2022; 40: 1500–1508. https://doi.org/10.1038/s41587-022-01334-x

[21] Margiotta F, Lucarini E, Toti A, Curti L, Masi A, Mello T, et al. Gut microbiota dysbiosis affects intestinal sensitivity through epithelium-to-neuron signaling: novel insights from a colon organoid-based model to improve visceral pain therapy. Gut Mi-

crobes. 2025; 17: 2547029. https://doi.org/10.1080/19490976.2025.2547029
[22] Yano JM, Yu K, Donaldson GP, Shastri GG, Ann P, Ma L, et al. Indigenous bacteria from the gut microbiota regulate host serotonin biosynthesis. Cell. 2015; 161: 264–276. https://doi.org/10.1016/j.cell.2015.02.047
[23] Mandić AD, Woting A, Jaenicke T, Sander A, Sabrowski W, Rolle-Kampcyk U, et al. Clostridium ramosum regulates enterochromaffin cell development and serotonin release. Scientific Reports. 2019; 9: 1177. https://doi.org/10.1038/s41598-018-38018-z
[24] Reigstad CS, Salmonson CE, Rainey JF, 3rd, Szurszewski JH, Linden DR, Sonnenburg JL, et al. Gut microbes promote colonic serotonin production through an effect of short-chain fatty acids on enterochromaffin cells. FASEB Journal: Official Publication of the Federation of American Societies for Experimental Biology. 2015; 29: 1395–1403. https://doi.org/10.1096/fj.14-259598
[25] Du Y, Fan C, Song X, Teng C, Zhang Z, Zhang J, et al. Gut microbiota and metabolite features in NSCLC nude mouse models of subcutaneous tumor and leptomeningeal metastasis: a microbiome-metabolome combined analysis. Frontiers in Cellular and Infection Microbiology. 2025; 15: 1616695. https://doi.org/10.3389/fcimb.2025.1616695
[26] Tzur Y, Dubnov S, Madrer N, Bar A, Nadorp B, Mishra N, et al. Ribosomal protein L24 mediates mammalian microRNA processing in an evolutionarily conserved manner. Cellular and Molecular Life Sciences: CMLS. 2024; 81: 55. https://doi.org/10.1007/s00018-023-05088-w
[27] Knight JRP, Vlahov N, Gay DM, Schuhmacher AJ, Saur D, di Tomaso E, et al. Rpl24Bst mutation suppresses colorectal cancer by promoting eEF2 phosphorylation via eEF2K. eLife. 2021; 10: e69729. https://doi.org/10.7554/eLife.69729
[28] Zhou F, Roy B, von Arnim AG. Translation reinitiation and development are compromised in similar ways by mutations in translation initiation factor eIF3h and the ribosomal protein RPL24. BMC Plant Biology. 2010; 10: 193. https://doi.org/10.1186/1471-2229-10-193
[29] Wei N, Wu X, Yu Y, Zhou H, Cui K, Zhao X, et al. CD146 promotes EMT-mediated migration and invasion of NSCLC via PI3K/Akt signaling pathway. Frontiers in Bioscience-Landmark. 2024; 29: 140. https://doi.org/10.31083/j.fbl2904140
[30] Sui H, Xu H, Ji Q, Liu X, Zhou L, Song H, et al. 5-Hydroxytryptamine receptor (5-HT1DR) promotes colorectal cancer metastasis by regulating Axin1/β-catenin/MMP-7 signaling pathway. Oncotarget. 2015; 6: 25975–25987. https://doi.org/10.18632/oncotarget.4543
[31] Tu RH, Wu SZ, Huang ZN, Zhong Q, Ye YH, Zheng CH, et al. Neurotransmitter Receptor HTR2B Regulates Lipid Metabolism to Inhibit Ferroptosis in Gastric Cancer. Cancer Research. 2023; 83: 3868–3885. https://doi.org/10.1158/0008-5472.CAN-23-1012
[32] Li B, Elsten-Brown J, Li M, Zhu E, Li Z, Chen Y, et al. Serotonin transporter inhibits antitumor immunity through regulating the intratumoral serotonin axis. Cell. 2025; 188: 3823–3842.e21. https://doi.org/10.1016/j.cell.2025.04.032
[33] Tone M, Tahara S, Nojima S, Motooka D, Okuzaki D, Morii E. HTR3A is correlated with unfavorable histology and promotes proliferation through ERK phosphorylation in lung adenocarcinoma. Cancer Science. 2020; 111: 3953–3961. https://doi.org/10.1111/cas.14592
[34] Tsay JJ, Wu BG, Sulaiman I, Gershner K, Schluger R, Li Y, et al. Lower Airway Dysbiosis Affects Lung Cancer Progression. Cancer Discovery. 2021; 11, 293–307. https://doi.org/10.1158/2159-8290.CD-20-0263
[35] Harding SD, Armstrong JF, Faccenda E, Southan C, Alexander SPH, Davenport AP, et al. The IUPHAR/BPS Guide to PHARMACOLOGY in 2026. Nucleic Acids Research. 2026; 54: D1446–D1456. https://doi.org/10.1093/nar/gkaf1067
[36] Zuo P, Haberer LJ, Fang L, Hunt TL, Ridgway D, Russo MW. Integration of modeling and simulation to support changes to ondansetron dosing following a randomized, double-blind, placebo-, and active-controlled thorough QT study. Journal of Clinical Pharmacology. 2014; 54: 1221–1229. https://doi.org/10.1002/jcph.322
[37] Gershon MD. Targeting serotonin transporter boosts tumor-fighting T cells. Cell. 2025; 188: 3631–3632. https://doi.org/10.1016/j.cell.2025.06.012
[38] Xu Y, Tao Y, Pan H, Wang Z, Wang H, Luo Q. Microbiome modulation in lung cancer immunotherapy: unveiling the role of respiratory and gut microbiota in the PD-1/PD-L1 response. Frontiers in Bioscience-Landmark. 2025; 30: 41531. https://doi.org/10.31083/FBL41531